Automation in Construction 41 (2014) 1–14

Contents lists available at ScienceDirect

Automation in Construction

journal homepage: www.elsevier.com/locate/autcon

Mobile 3D mapping for surveying earthwork projects using an Unmanned Aerial Vehicle (UAV) system

Sebastian Siebert [a], Jochen Teizer [b,*]

[a] Bickhardt Bau Aktiengesellschaft, Industriestraße 9, 36275 Kirchheim, Germany
[b] RAPIDS Construction Safety and Technology Laboratory, School of Civil and Environmental Engineering, Georgia Institute of Technology, 790 Atlantic Dr. N.W., Atlanta, GA 30332-0355, USA

ARTICLE INFO

Article history:
Accepted 31 January 2014
Available online 19 February 2014

Keywords:
Global positioning system (GPS)
Laser scanning
Photogrammetry
Robotic total station (RTS)
Robotic total station (RTS)
Airplane and helicopters
Remotely piloted vehicles (RPV)
Unmanned aerial vehicle (UAV) systems (UAS)
3D range point cloud generation and mapping
Autonomous vision-based infrastructure sensing
Efficiency, productivity, and safety in geomatics and surveying

ABSTRACT

Unmanned Aerial Vehicle (UAV) systems as a data acquisition platform and as a measurement instrument are becoming attractive for many surveying applications in civil engineering. Their performance, however, is not well understood for these particular tasks. The scope of the presented work is the performance evaluation of a UAV system that was built to rapidly and autonomously acquire mobile three-dimensional (3D) mapping data. Details to the components of the UAV system (hardware and control software) are explained. A novel program for photogrammetric flight planning and its execution for the generation of 3D point clouds from digital mobile images is explained. A performance model for estimating the position error was developed and tested in several realistic construction environments. Test results are presented as they relate to large excavation and earth moving construction sites. The experiences with the developed UAV system are useful to researchers or practitioners in need for successfully adapting UAV technology for their application(s).

Published by Elsevier B.V.

1. Introduction

Until recently, Unmanned Aerial Vehicles (UAV), Unmanned Aerial Systems (UAS), Remotely Piloted Vehicles (RPV), or also often known as drones, were mostly developed and used for military applications. These systems are remotely-controlled aircrafts or helicopters. They are equipped with precision sensors, for example, inertial motion units (IMU) and gyroscopes, for recognizing the alignment and position of the aircraft. A microcomputer makes the autonomous navigation without much manual involvement of a pilot possible. Due to the cost and size of these sensors, a non-military use and especially smaller UAV systems have not been feasible for many commercial applications. With the recent availability of highly accurate and low-cost Global Positioning Systems (GPS), the possibility opened up to maintain a UAV system's position in a global reference system nearly everywhere in the world and in real-time. However, selective availability of such GPS signals had prevented most commercial applications. It was until the mid-1990 when the accuracy of GPS for commercial applications dropped to just a few meters [1]. The development of cost-efficient and light gyroscopes to measure alignment and orientation primarily for smart telephones enabled many hobby modelers to update their airplane or helicopter models to a fully functional UAV. This is also a reason why most of the UAV developers gained their first experiences with model aircrafts.

With the arrival of precise GPS and gyroscope technology the performance, especially the payload, endurance, and flexibility for diverse and reliable application of UAV systems, significantly improved. Most recently, light-weight digital photo or video cameras converted autonomous UAV systems to highly mobile sensor platforms. However, few applications in civil engineering have yet been fully explored although they promise to provide more cost- and task-efficient ways to conventional approaches. For example, surveying applications are relying mostly on labor-intensive GPS, Robotic Total Station (RTS), laser scanning, and tachymetry. In addition, there are air- or space-borne technologies available, but their selection depends on the terrain and size of the area that must be surveyed. They are limited in range, very labor intensive and costly, have potentially high measurement errors, and are time consuming to perform.

UAVs offer a potential solution to these concerns. Once UAV technology proves to be accurate and reliable it might assist or replace a specific segment in surveying applications. Although several researchers have previously introduced UAV technology to civil engineering applications [2], its performance in the construction environment has yet to be scientifically explored and evaluated.

* Corresponding author.
E-mail address: teizer@gatech.edu (J. Teizer).

0926-5805/$ – see front matter. Published by Elsevier B.V.
http://dx.doi.org/10.1016/j.autcon.2014.01.004

The potential range of surveying tasks which UAV technology is able to perform is shown in Fig. 1. The worldwide use of UAVs is regulated by the specific national federal administrations. For safety and security reasons commercial UAV use is typically restricted to flights within line-of-sight (LOS) of an operator. Typically the operator is referred to a *pilot*. It ensures that a pilot has permanent control and interaction in case of unexpected events, for example, other aircraft(s) operate nearby or changes happen to any of the environmental conditions which might influence the UAV's flight conditions, such as wind parameters.

2. Recent UAV research within civil engineering applications

In recent years, researchers have been showing growing interest in utilizing UAV systems for diverse non-military purposes. They are used in forest and agricultural applications [3,4], autonomous surveillance [5,6], emergency and disaster management [7], traffic surveillance and management [8–10], photogrammetry for 3D modeling [2,11,12], remote-sensing based inspection systems [13], and many more domains. This is mainly due to the low cost, fast speed, high maneuverability, and high safety of UAV systems for collecting images. UAVs are already a reliable replacement over satellites and manned vehicles. Moreover, they have overcome the disadvantage of low flexibility and high cost of aerial imagery.

To date, much research has been conducted in UAV photogrammetry [2,11,12,14–16] for 3D mapping and modeling. For example, Hudzietz and Saripalli [14] have successfully employed structure from motion (SfM) techniques for the reconstruction of aerial imagery from landscapes. Aerial photography was ultimately converted into 3D models of the terrain. They showed that a UAV used as a platform for collecting images offers large-scale terrain modeling very cost-effectively, efficiently, and accurately. However, little research is found in the literature focusing on the application of UAV-based systems in civil engineering applications. Hudzietz and Saripalli [14], for example, only reported results on ground-based tests from an unknown distance which makes the evaluation of measurement errors in actual field trials difficult.

Jizhou et al. [17] designed and implemented an algorithm for 3D reconstruction of city buildings from multiple images using a single UAV. The UAV had the ability to derive both geometry and texture information from UAV images. Lately, UAV has been exploited for capturing images of a building of interest from multiple different perspectives, which resulted in a 3D model of the building [18]. This particular experiment was done by a Falcon 8 octocopter from Ascending Technologies equipped with a high-resolution consumer camera as the data acquisition sensor. The final 3D reconstruction was computed offline. They showed that the accuracy of the obtained model was comparable with the results of sensing with Light Detection and Ranging (LiDAR). Among the many of the existing UAV references, this reference fails to explain the methods (terrestrial or LiDAR) and error rates in greater detail.

Metni and Hamel [19] investigated the usability of UAV systems for the monitoring and maintenance of bridges and structures and presented a novel control law of a UAV under some practical restrictions which are based on computer vision. Rathinam et al. [20] addressed the problem of autonomous UAV-based monitoring of linear structures such as pipelines, roads, bridges, canals, and power generation grids. A closed-loop control algorithm was developed for detecting linear structures locally using visual recognition techniques in real-time.

Further potential applications of UAV remote sensing are geologic hazard assessment of gas and oil pipelines [21]. Zhang and Elaksher [22] presented a UAV-based imaging system for the 3D evaluation of rural road surface distresses. For this purpose, a system consisting of an inexpensive helicopter equipped with a camera for unpaved road data acquisition, a global positioning system (GPS) receiver and an inertial navigation system (INS) for navigating the helicopter were utilized. Their proposed image processing algorithm produced a complete 3D model of the surface distresses which enabled measurement of the distresses such as potholes and ruts in 3D. Recently, the usability of small-scale UAV systems as a safety inspection tool on construction sites has been proposed by [23]. They suggested the employment of an inexpensive quadcopter equipped with a camera. The proposed UAV should provide a safety manager with real-time access to videos or still images of construction sites. Noteworthy, they designed the system to be controlled with an easy-to-use large-size interface system using an iPad, and as a result, safety managers could interact with workers at ease. Their heuristic experiments showed that UAV systems could have potential benefits to safety managers on construction sites. However, their conceptual approach was not validated in the field.

3. Definition and types of UAV systems

Many UAV systems exist today and have commercial applications. Many UAVs are built on existing model airplanes or helicopters. The exceptions are military drones that are quite expensive to build and operate and thus do not offer a cost-effective alternative for many users in the civil application domain, including construction engineering and

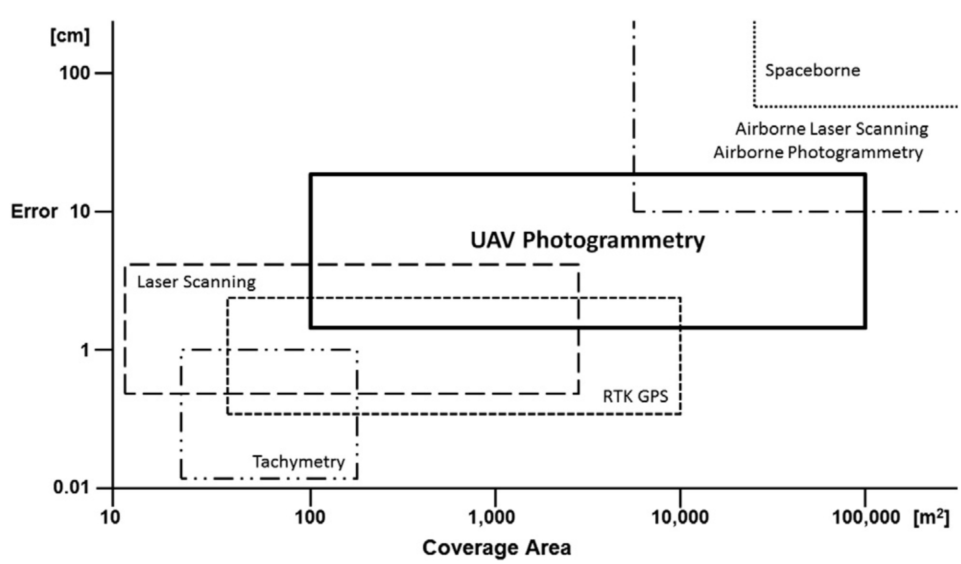

Fig. 1. Potential UAV application areas in surveying tasks.
Modified and updated after [2].

management. Many of the UAV systems that find application in the civil domain offer already cost- and time-competitive alternatives to conventional surveying applications. The purchase price of UAVs has dropped rapidly. Maintenance costs are also very small. Its size, payload, range, and operating mode are typically the main criteria a user defines before investing in a UAV system. Answering the following questions might help in the selection of a UAV system:

- What is the size of the area to be surveyed?
- What is the flying altitude the UAV needs to operate?
- What camera system and what camera mount system (aka. gimbal) is needed?
- Are third party persons working in the area?
- Are other physical obstacles present?
- What take-off/landing space is available?

Before answering these questions, background knowledge on UAV is indeed needed. UAVs, like planes or helicopters, can be categorized by its structure and by its type of taking-off/landing. The following explains the advantages and limitations of four of the main UAV types. Table 1 summarizes the UAV categories into:

- *Horizontal flying self-propelled fixed-wing aircrafts:* They are capable of flight using wings which generate lift caused by the vehicle's forward airspeed and the shape of the wings. They are distinct from rotary-wing aircrafts in which a motor provides forward thrust from an engine. Most unmanned fixed-wing aircrafts are easy to fly by a pilot remotely or automatically/computer-controlled. They are often called remotely piloted vehicles (RPV). Although fixed wing aircrafts offer high efficiency and range to survey large areas at relatively low building and operating cost, a take-off and landing strip is required.
- *Vertical starting systems:* They often use rotor blades to lift a platform. Helicopters have a tail rotor to balance the torque of the main rotor and subsequently use more energy while offering potentially less flying time. Their main advantage though is high flexibility in operation and taking off/landing.
- *Airships:* Airships can also take-off and land vertically. Their flight time and range is long. They have the ability to operate in limited and safety critical areas. Depending on their size, they can carry heavy payloads, but are more exposed to winds, may need a longer setup times, and may have higher running costs than other UAV types.
- *Multicopters:* They are a special type of a rotary wing aircraft. The torque does not create energy loss due to the rotors rotating in the opposite direction. The high efficiency of helicopters has yet to be met because of its reliance on electronic motors and batteries. Their main advantage is the ease of operation, high flexibility, and stability. Most recent models offer a payload of up to 5 kg and can carry complex and heavy surveying systems, such as a single-lens reflex (SLR) cameras. Commonly used multicopters have at least four rotors (quadrocopter), but can have more (hexacopter or octocopter) for redundancy purposes. Purchase cost and maintenance typically increases respectively, although an increase in safe operation and payload are sometimes important factors to consider. They all work using the same operating principle that a quadrocopter has, but additional rotors may offer redundancy to protect the investment. Flying a multicopter requires an experienced pilot, but is relatively easy, requires little maintenance, and comes generally at low operating and maintenance cost. Multicopters can also be programmed to fly autonomously along pre-programmed waypoints. Software exists for this purpose.

For many years now UAV systems have flown autonomously using the Global Navigation Satellite System (GNSS). Their sophistication has allowed longer periods of flight time and covering larger areas. Disadvantages are flexibility and potentially high exposure to wind loads.

4. Design, components, and assembly of a quadrocopter

The developed UAV system was specifically designed to successfully complete surveying tasks in civil engineering applications. The system is based on the quadrocopter principle. Fig. 2 displays the main components of the UAV system that was built. Quadrocopters have distinct advantages compared to other existing UAV approaches. Some of the advantages are its low purchase, operation, and maintenance costs, its flexibility to operate (take-off and land) in very small surveying assignments, the easiness to steer it reliably in autonomous and pilot mode, and to keep it under control when harsher ambient environments exist, for example, strong winds. Some of its main limitations are limited range (typically a few hundred meters) and flight time (up to 20-30 min). Many limitations might be less critical to a user because many federal regulations allow line-of-sight (LOS) operation of UAVs only. The developed UAV obtained a special license to operate it for extended ranges.

The design of the developed quadrocopter is based on components of the Mikrokopter Quad XL [24]. It was assembled with four brushless electrical motors and 30.5 cm long carbon fiber propellers. Its total size in diameter is 1 m. The quadrocopter is able to produce an absolute thrust of 9 kg. It's empty (without battery and camera) and gross weight is 1 and 2.6 kg, respectively. The lithium-polymer battery weighs 0.6 kg and provides 14.8 V at a capacity of 6600 mAh. A payload of 1.5 kg can be added. Some of it was used to mount a Sony NEX5N (16 mm fixed focal length, 16.1 MP per image) camera system.

The frame of the quadrocopter is made out of lightweight materials such as aluminum and carbon fiber reinforced plastic. It has space for the motors, battery, electronic parts, and the camera mount (aka. gimbal). The Flight Control Unit (FCU) is the core part of any UAV. It is able to process and implement the input commands from the pilot or the autonomous navigation routine into certain navigational tasks. The Inertial Measurement Unit (IMU) is designed to recognize the actual alignment, acceleration, and barometrical altitude. The four brushless motor controllers receive their commands from the FCU to trigger the rotational speed of the motors. The FCU is also directly connected with a low cost differential GPS receiver and a magnetic compass. It is designed to extend the navigational capabilities of the quadrocopter, for example, functions become possible like 'position hold', 'coming home', and 'flight according to pre-identified waypoints'.

The flight trajectory data for a waypoint route is typically stored in a digital file that is submitted to the UAV with a wireless data upload link from a ground control station, a mobile computer or smartphone. Thanks to a XML-based file structure of the waypoint file it is possible to create a waypoint route with an external software solution. Equipped with a differential GPS receiver, the quadrocopter was able to follow autonomously a pre-defined 3D flight trajectory of up to 100 waypoints.

Table 1
Comparison of advantages and limitations of existing flight systems (* can be limited by federal or state regulations).

Aircraft Type	Efficiency and range*	Flexibility and maneuverability	Weather dependency	Payload	Safety	Complexity and simplicity	Running costs	Setup time
Airships	Very good	Average	Poor	Very good	Good	Good	Poor	Poor
Fixed wing aircraft	Very good	Poor	Good	Good	Average	Average	Average	Average
Helicopters	Average	Very good	Good	Very good	Poor	Poor	Average	Good
Multicopters	Poor	Very good	Good	Average	Average	Good	Very good	Very good

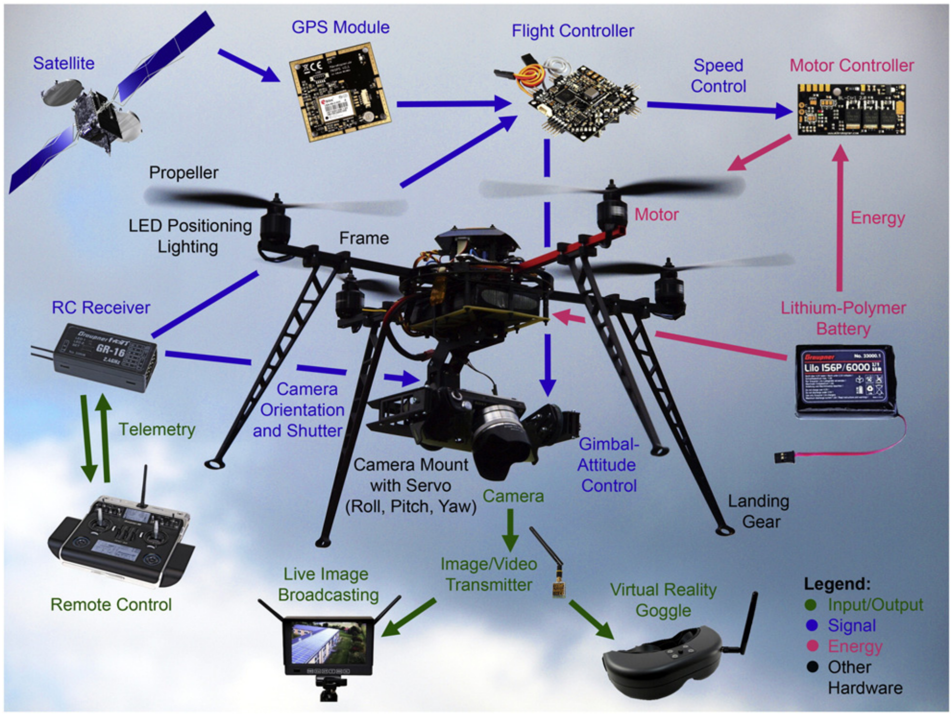

Fig. 2. The main components of the developed UAV system: data and power flow.

The current waypoint file specifies global position, flying altitude above ground, heading, speed, and the external control for pitch and triggering of the camera. A user can automatically generate the waypoints according to pre-defined settings, for example for flying the UAV in a circle or other more complex pattern.

It also allows specifying the time the quadrocopter spends at a waypoint location and the required accuracy before the camera takes a photo. Photos are normally taken on the fly. The camera mount on the bottom of the quadrocopter includes two servo motors which control the pitch and roll angles of the camera. This allows the camera to stay in a nadir position during the flight. The camera shutter is controlled with an infrared-trigger device that is connected to the FCU.

In the current design, the quadrocopter is able to stay about for 18 min in the air and can travel a total distance of about 4 km at an average speed of 4 m/s. The maximum flying altitude is not limited, but the typical operational altitude is below 100 m. Although these technical characteristics are available, the surveying assignments the quadrocopter was given in this research required it to travel only about 400 m at a time and at an altitude of about 70 m. The quadrocopter can be both manually controlled or put in an autonomous flight mode. A commercially-available 2.4 GHz transmitter (as it is used to steer many model aircrafts or helicopters) was used for manual control purpose. An 868 MHz data link provides the possibility to maintain real-time flight information and wireless waypoint transmitting.

Essential UAV building expertise for the hardware assembly was necessary, which may require assistance by a professional. The modular UAV design allows adding or replacing quadrocopter components as a user requests, for example, camera mount and wireless data signal transmission. This is particularly helpful in optimizing the design for practical uses in civil engineering applications. The total hardware cost is estimated to a few thousand dollars (about $8000), thus offering a potentially attractive investment-return opportunity for a user.

5. Flight path planning and data collection process

At an early research stage it was realized that commercially-available flight preparation tools were insufficient in handling photogrammetric surveying applications. A new methodology was designed (see Fig. 3) based upon the Mikrokopter Flight Planning Tool (MK FPT). It was modified to minimize the manual effort in the flight planning process. The modified version of the computer program addressed some specific aspects of aerial photogrammetry for surveying applications in civil engineering, for example, overlapping of photo imagery to guarantee the appropriate overlapping coverage. All that is left for a pilot is to select the region of interest (survey area) on an interactive map, camera model, photo size and resolution, flight altitude above ground, flight speed, and the longitudinal and traversal coverage area of each photo (see Fig. 4). The developed flight planning software uses these parameters to compute a full flight plan consisting of the waypoints where the quadrocopter takes along its flight path the photos automatically. The file format that stores the flight plan is .WPL. As mentioned before, up to 100 waypoints can be entered in a user-interface with very little manual effort. The developed interface allows the user to click on a satellite map to define the area of interest with a polygon. Based on a preset resolution, an optimized flight path is automatically generated. It is important to note, that the developed interface is unique and in addition to existing flight path planning software. Fig. 4 shows in an example that in addition to the 14 waypoints that were automatically identified for an area of 80 by 100 m, the interface allowed to specify further camera parameters. These are: longitudinal and traversal coverage of 70 and 40%, respectively. The area a single photo covered a constant flying altitude of 50 m represents 73 by 48 m on the ground and at the ground resolution of 1.49 cm per pixel.

The following flight process was developed: (1) prepare UAV for flight, for example, check its hardware including frame, motors, propellers, battery, sensors, and availability of signal, (2) turn on the (photo) camera, (3) upload the waypoints for the flight path, (4) check the environmental conditions including surrounding airspace, wind, human hazards, and (5) turn quadrocopter on, lift it off the ground manually, and switch to autonomous flight mode. After take-off, the quadrocopter is following its preset tasks autonomously. At each waypoint the quadrocopter takes a photo. In case of an unexpected event, a manual intervention is possible at any time. When the last waypoint is reached, the UAV returns automatically to its lift-off location by switching to the

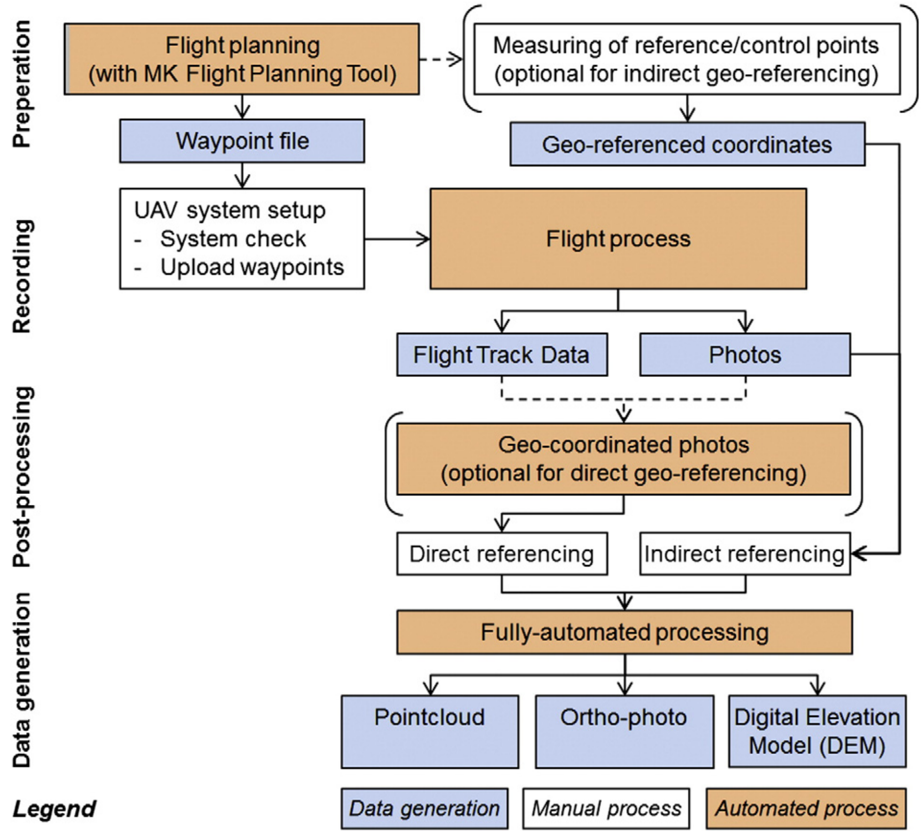

Fig. 3. UAV flight methodology: preparation, recording, post-flight data processing, and information generation.

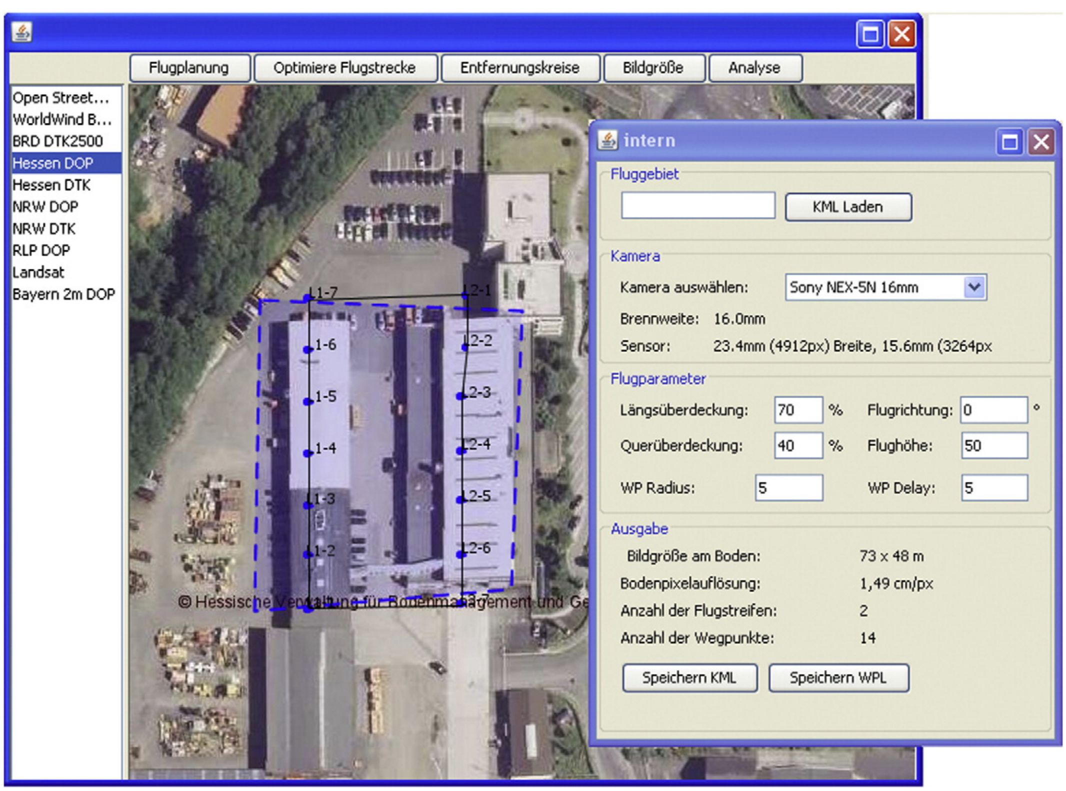

Fig. 4. The developed UAV flight path planning software interface: coverage area (dashed lines), flight path (dotted straight lines) according to waypoints (dots), and user interface to select UAV and camera parameters.

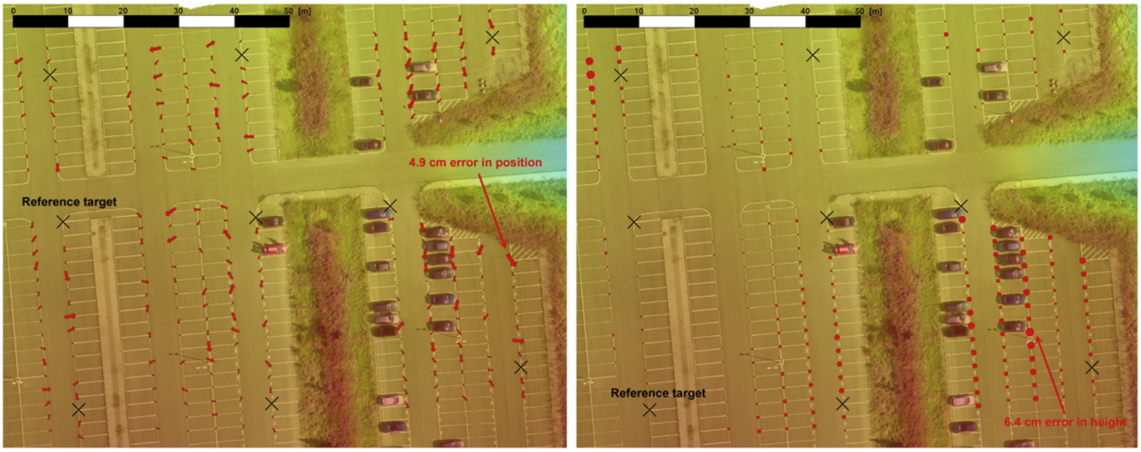

Fig. 5. Results of the 2012 UAV error measurements: arrows indicating the size and orientation of errors in position (left) and circles indicating the size of errors in height (right).

"coming home" mode. The landing can be performed either manually or automatically. The data acquisition is complete. If the size of the survey area is too large for one flight, additional flights can be performed and data merged seamlessly.

6. Photogrammetric data processing and generation of 3D point clouds

Photogrammetric data processing is needed to generate a geo-referenced 3D point cloud from the unordered, overlapping, and airborne image collection of the surface. Existing Structure from Motion (SfM) algorithms automatically extracted features in the images, for example, contour lines, edges, and feature points. Homologous areas, interior and exterior orientations were computed in a bundle adjustment. The Exchangeable Image Format (Exif) metadata from each digital image further provided approximate values for the focal length and image size.

A detailed review on how to generate 3D point clouds from photo imagery can be found in related literature by Lowe [25] and Snavely et al. [26]. They applied SIFT (Scale Invariant Feature Transform) for key-point detection. Furukawa et al. [27] proposed a multi-stereo-view approach for large unorganized datasets. Furukawa and Ponce [28] presented an algorithm for generating referenced 3D point clouds that are based on the computation of rectangular patches in overlapping areas of adjacent images.

A commercially-existing software solution by AgiSoft PhotoScan [29], called PhotoScan, establishes the relation between the unordered image data collection. This software has been recently optimized for the use with UAV. The software's professional edition allows to geo-reference the results in a specific coordinate system. It exports these to a digital elevation model or orthophoto. The recommended computer processing requirements for such large data gathering projects with more than 100 images are a 64-bit operating system with at least 16 GB RAM.

The data processing is not complicated. First, all aerial images were imported from the camera to the computer. It was necessary that the images have adequate overlap between each other. From the Exif metadata, their approximated interior orientation (focal length and image sensor size) was determined. Thereafter, a step-wise processing of the image collection began: (1) align photos, (2) build geometry, and (3) build texture (if required). Each step gave several possibilities to adjust parameters, which have influence on the accuracy and structure of the results and the processing time.

It is generally possible to export the results as a colored point cloud, a digital elevation model with matched texture, or an orthophoto. An automatically generated report assesses the quality and accuracy to each step in the data processing process. It is essential to geo-reference the data for further use in surveying applications. This task can be completed in two different ways within the software PhotoScan: direct and indirect geo-referencing.

Direct geo-referencing can be achieved by using time-stamped GPS data which is recorded during the flight. Synchronization of the internal camera time and GPS time is achieved automatically. The exposure position of the image will be integrated in the Exif data as geographical coordinates in the WGS84 format. PhotoScan integrates all data and makes an adjustment to the exterior orientation of the images. As a result, a point cloud is transferred to the given coordinate system.

Indirect geo-referencing can be applied by measuring reference targets that were deployed on the ground in the area of interest before the flight. These targets must be clearly visible in the images. Should targets not be available, it is also possible to use existing features in the environment which are fixed, for example, manhole covers or road markings. These reference points must be surveyed with a suitable survey method, for example, differential GPS or tachymetry. During the data processing process it is also necessary to manually identify the reference points in the model provided by the software. The measured coordinates of the targets will be referenced to the model. Accordingly, the complete model will be geo-referenced using a spatial transformation. At least three reference points are needed for this process, but it is recommended to use significantly more.

Direct geo-referencing offers the advantages that no ground-based surveying and neither manipulation of the 3D point cloud are necessary. It is faster than indirect geo-referencing. However, indirect geo-referencing can take full advantage of using the GPS data that was recorded during the flight and relate it easily to the GPS data which was collected in the field. As such, the user has to decide if the final product of a referenced point cloud should be achieved faster (in such case, preference should be given to a direct geo-referencing method) or if higher accuracy is required (then, an indirect geo-referencing method should be used). Existing commercially-available photogrammetric data processing software can perform the referencing task of 100 images taken during a UAV flight within about three hours or less.

Table 2
Comparing the errors of a UAV operating under new parameters in the same test bed environment.

	Neitzel et al. 2011 [30]	Siebert and Teizer in 2012
Software	Agisoft PhotoScan Standard 2010	Agisoft PhotoScan Professional 2012
Flying altitude (resolution)	30 m (0.7 cm/pixel)	50 m (1.2 cm/pixel)
Reference points	6	9
Image count	99	49
Average positional error	5.6 cm	0.6 cm
Average height error	−2.5 cm	−1.1 cm

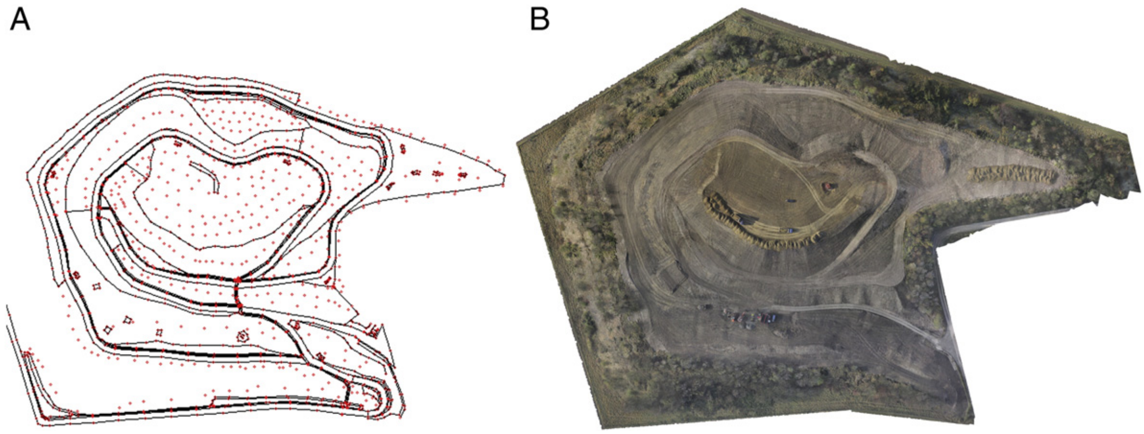

Fig. 6. Traditional ground-based RTK GPS survey using a few hundred individual points from a manual survey and (b) photogrammetric surveying using the UAV to collect autonomously millions of color-coded measurement points and present them in an orthophoto.

7. Error analysis and evaluation in a test bed environment

For the use in surveying applications an absolute accuracy analyses of the point cloud is mandatory. Preliminary results from a first approach were published by one of the authors in [16 and 30]. Their purpose was to compare several low cost and free software solutions for SfM under similar conditions. The error of their UAV and data processing software solutions was measured using a test bed environment in the size of 100 by 150 m. For an absolute error analysis, nearly 500 corner points of pavement markings on a parking lot were surveyed in position and height using a traditional tachymetry surveying approach (using a Robotic Total Station). These control points were measured as UTM (Universal Transverse Mercator) coordinates on the WGS84 ellipsoid with an approximately accuracy of 1 cm in position and height. For the first approach, six of these control points were used for the transformation of the UAV results. Afterwards, the remaining control points of the transformed point cloud were manually measured and compared. An average positional error of 5.6 cm and a height error of 2.5 cm were measured for the results using the software PhotoScan. Further results reported show that the errors largely depended on the topography of the test bed area.

The presented UAV error analysis used the same test bed for evaluation of its measurement error. The UAV flew at multiple different heights. In the earlier experiments the camera attached to the UAV took 99 photos at 30 m height at a ground resolution of 0.7 cm per pixel and 49 photos at 50 m at a ground resolution of 1.2 cm per pixel. The point cloud resulting from the images at 30 m height was selected because it had initially a higher ground resolution. Later experiments showed, however, that a flying altitude of 50 m is preferred over lower flying heights due to the fact that individually taken photos have more overlap with each other.

New experiments in the same test bed were conducted using additional and modified features of the software functions. These were integrated geo-referencing, advanced export functions, script support, optimized camera parameters, and point clouds referenced with the help of measured target points. The new experiment led to a decrease in the errors using the same baseline data. The new measurement also required fewer photos from a flying altitude at about 50 m, since the images taken at the new altitude had more overlapping areas with each other. Finally, nine instead of six reference target points on the ground were used (see “x” in Fig. 5). In brief, adding more features to the referencing process significantly contributed to a reduced error. The optimization of the point cloud is represented by minimizing the sum of re-projection and reference coordinate misalignment errors.

The error analysis method used the target vs. actual comparison. The target coordinates (position and height) were measured using the tachymeter. The actual coordinates were based on the surface model which was generated through the photogrammetric approach. The developed software allowed direct comparison of both approaches in a table-based format. The average positional and height errors are the result of all target/actual-comparisons after eliminating outliers. Outliers in the test bed were caused by cars which obstructed the view of several control points on the asphalt surface of the parking lot. They were removed manually. As shown in Table 2, the average positional error was reduced to 0.6 cm and the average height error was reduced to −1.1 cm. The maximum error of a single point was 4.9 cm in position and 6.4 cm in height. Improvements in results can be expected when using professional series UAV design and higher-resolution. A modern Multicopter system has a much more accurate flight trajectory and can lift cameras and mobile sensors with up to 3 kg [24]. In comparison the UAV used for this test bed was an octocopter designed in 2009 and equipped with a small digital compact camera (Canon IXUS100 IS).

The errors in the experiments of one of the authors in 2012 were visualized and compared to the ones of Neitzel et al. [30] performed in 2010. The thickness of the arrows in Fig. 5 displays the size of the error at a given location (marking stripes on the parking lot). Compared to the previous results, the positional error is with an average of 0.6 cm noticeable smaller and shows no systematic distortion. In addition, the height errors in the bottom right area of the test bed area can be seen. Similar to the previous publication, reasons why better results were achieved compared to the earlier approach can be: (a) more overlapping photos were taken, (b) geo-referencing the test bed directly in the photogrammetry software, (c) measuring the control points directly in the photogrammetry software, and (d) optimizing the camera parameters with the help of reference points [29].

Table 3
Comparison of RTK GPS vs. UAV survey results.

Survey method		RTK GPS survey	UAV photogrammetric mapping
Coverage area		60,000 m^2	60,000 m^2
Time needed	Preparation	30 min	40 min
	Recording	540 min	15 min
	Evaluation/ Processing	60 min	150 min
	Overall	630 min	205 min
Point count		1800	5,500,000 (not all might be used)
Point density		0.03 points/m^2	92 points/m^2
Result		Interpreted surface model	Dense surface model, orthophoto

8. UAV performance measurements and results

8.1. The economics of applying a UAV to survey a landfill

The utilization of UAVs in the photogrammetric data collection of landfills and surface mines promises to have very good applications. Aside from safety and security issues, two goals are important to practitioners in the adoption of UAV to existing surveying approaches: (a) cost-effectiveness and (b) highly accurate measurements. A timely gathering of a mine's or construction site's as-built status is necessary and typically requires frequent and resources intensive surveying. Low vegetation in such environments, especially in mines, allows effective use of a UAV since surface data collection is unobstructed and analysis requires little manual interference. Another advantage of UAV is that surveyors very often operate in a dangerous environment. They are, for example, exposed to leading edges or highly sloped surfaces in mines. Falls or sliding can be the result leading to injury or more likely, to a fatality. Other dominant hazards for surveyors-on-

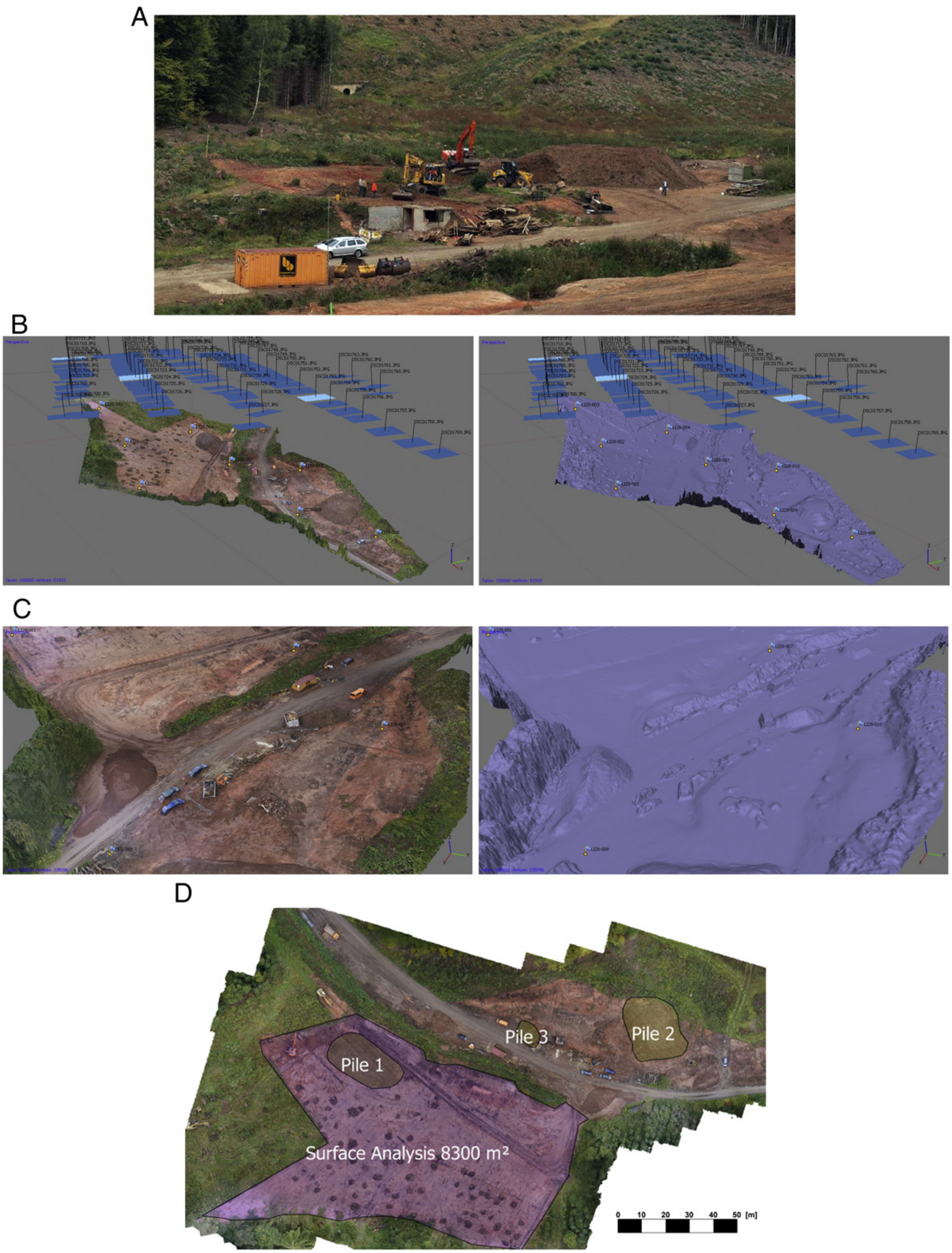

Fig. 7. Application of the UAV in earthmoving operations during a road construction project.

foot are proximity-related exposures to nearby operating heavy equipment which must be strictly avoided [31–35]. However, accurate measurement of leading edges and line work is crucial in successfully operating landfills and mines since they are used to quantify volumes and determine as-built drawings.

A landfill nearby the City of Magdeburg, Germany, was selected as one of the test sites for the first application of the developed UAV. The goal of the construction project was to re-cultivate the topsoil and create a new surface profile for an area of 200 by 300 m. The landfill was unobstructed from vegetation or any manmade objects. Heavy construction equipment equipped with RTK GPS was utilized to maintain very high accuracy in the earthmoving operation. The job was divided into sections. At the end of every section detailed surveying was necessary and required to measure progress and accuracy of the work that had been performed.

A total of three photogrammetric measurements were conducted and compared to the conventional surveying technique that was also performed. The UAV's longitudinal and traversal coverage areas of each photo image were 60 and 40%, respectively. Its flying altitude was 75 m above the highest point in the entire terrain. The flight planning used the developed MK FPT. The data was analyzed using the Agisoft Photoscan Professional software. A total of eight ground-based reference points were used to compare the target/actual-data points.

The main objective of this measurement was to validate the goals set earlier: to measure the cost-effectiveness of the UAV approach and the size of its errors. Further goals were to understand the process better of using a UAV in civil engineering and surveying applications and to point out potential improvements in replacing ground-based personnel (e.g., safety and efficiency) and supporting (semi-) automated machine guidance (AMG) using survey-grade positioning and elevation data. In brief, the conventional ground-based (see Fig. 6, left image) and the UAV photogrammetric-based (see Fig. 6, right image) surveying approaches were compared.

The UAV took 64 pictures with an overlapping image rate of 60% longitudinal and 40% lateral. The computational processing time was approximately 30 min. The PC hardware (Intel Core i7, 64 GB RAM and Windows 7, 64 bit) processed about 100 pictures in 1 h. Exponentially more time would be needed for more pictures at a maximum of about 300–400 pictures per processing time.

Noteworthy additional observations (see Table 3) that go beyond error analysis and impact the performance of UAVs were noticed during the experiment and are presented:

- *Wind:* Due to the unobstructed area, stronger thermal winds caused air turbulences for the UAV. Some blurred photos had to be manually removed. One UAV data collection was canceled due to wind gusts of more than 40 km/h.
- *Obstacles:* Cameras mounted on the UAV recorded any in object in its field-of-view. Eventually larger volumes due to inclusion of temporary objects – for example pieces of equipment, temporary support structures, interlace storage or cut/fill locations, or a trench – might need to be removed/added manually as they should not count towards the final earthwork volume count. Such adjustment – as needed on a few occasions in the conducted experiment – was done manually and is already accounted for in the time calculation of Table 3. The results though did not change significantly.
- *Safety and security:* UAV operation in highly populated areas which are unsafe or unsecure for any bystanders (pedestrians or other traffic) or the UAV equipment itself needs to be avoided or might require special review.
- *Time:* The UAV required only 3% of the conventional RTK GPS-based data acquisition time and was able to always record the entire survey area. The UAV was therefore able to track the progress of the entire landfill at any time while RTK GPS data was only recorded in areas where construction progressed. However, evaluation of the UAV-generated photos for errors (blur and obstructions) required more time. Overall, the UAV photogrammetric mapping approach required about one third of the time a RTK GPS survey has taken (ratio depends on coverage area).
- *Area of coverage:* The main advantage of an orthophoto from the UAV is a geometrically corrected aerial photograph that is projected similarly to a topographical map. When viewed, an orthophoto displays true ground position with a constant scale throughout the image. This can be very helpful for field engineers for the direct measurement of distances, areas, and positions, and in particular when creating cross-sectional views or other terrain map information. For larger construction sites RTK GPS or conventional surveying approaches are simply not efficient enough and may only be used if the criteria for UAV use are not met, for example when obstacles such as trees that limit the field-of-view of a camera mounted on the UAV.
- *Point classification:* A main disadvantage of the UAV-based approach (and any other point cloud data acquisition) though is that it does not analyze the point cloud information automatically. The RTK GPS allows the use of standardized point codes that classify the type of point, for example, point belongs to trench or road. Thus to date, the point cloud data of the UAV must be manually annotated.

These and other findings were learned from operating the UAV on similar-type projects. They benefit or limit the application of the technology and direct further development that is necessary to enhance its performance. A particular recommendation is to use sufficient longitudinal and traversal coverage areas (at least 70 and 40%, respectively). Image blurs can be removed while increasing the overall point cloud density. Further optimization can be achieved when the camera's shutter speed is high. Proper flight planning through the use of permanent reference targets on identical areas minimizes data gathering since the marking, gathering, and collection of such points can be time and resource (labor) intensive tasks. Using eventually natural reference points may minimize this effort.

8.2. Application in earthmoving during road construction

Existing performance results relate mostly to optimal test bed scenarios and conditions. Measuring the error performance of a UAV system ultimately requires evaluation in a realistic field study. Various test sites under realistic conditions were selected to measure the error performance of the developed UAV system and to highlight its advantages and current limitations. A secondary objective of these field trials was to generate very dense 3D point clouds from aerial photogrammetry (orthophotos with more than 100 points per square meter). Ground truth data was measured using conventional survey techniques, for instance, processes which generate highly accurate surface models from differential GPS receivers and tachymetry. Since obtaining such models is time consuming and resource (personnel and instrument) intensive, the field user had in mind estimating large earth-volumes in excavation and hauling applications rapidly for potential later use in advanced productivity and progress monitoring applications. As earth volume estimates generated by a UAV-based surveying approach may differ from any conventional surveying method, greater interest was put on measuring the errors in the generated 3D surface models and earth volumes.

Table 4
Comparison of results to RTS and UAV survey applied to a larger excavation area.

Survey method		RTS survey	UAV-mapping
Coverage area		14,330 m^2	24,900 m^2
Time needed	Preparation	120 min	60 min
	Recording	420 min	15 min
	Evaluation/Processing	120 min	90 min
	Overall	660 min	165 min
Point count		350	More than 2,000,000
Point density		0.02 points/m^2	Up to 561 points/m^2

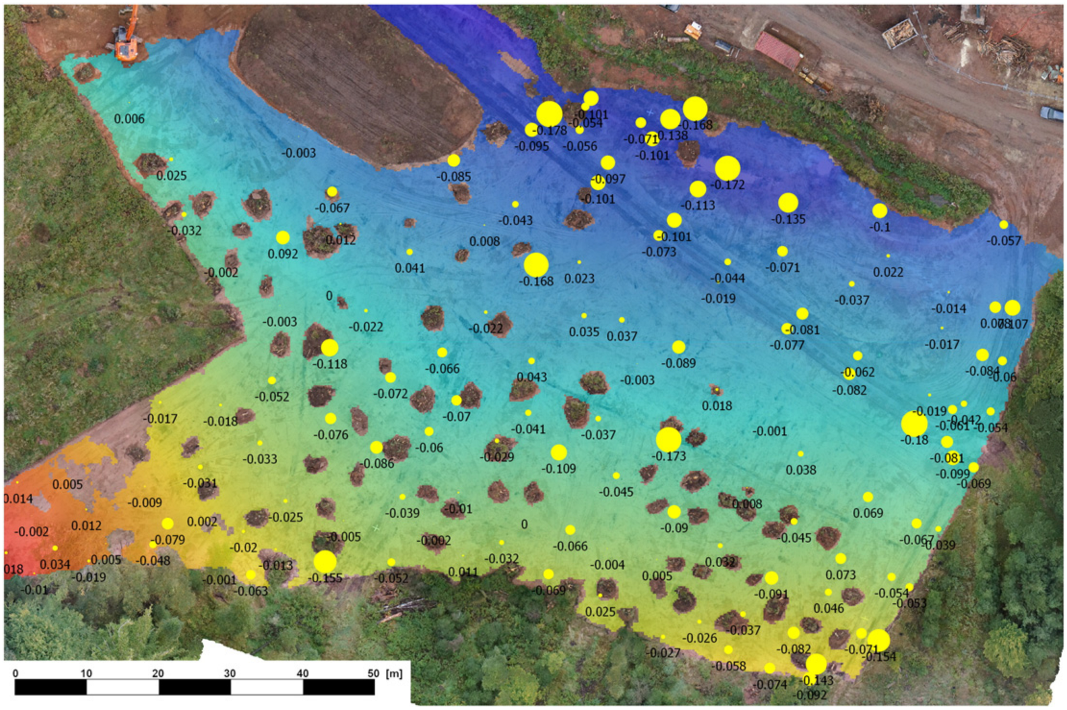

Fig. 8. Error location and size (in m) of the UAV-generated survey data set in a field-realistic environment.

The location of the test site was Friedewald, Germany. The widening of an existing highway required the removal of an old clay pigeon shooting range (see Fig. 7). Since such clay material is considered hazardous waste under German law, the site required specialized excavation and treatment before any of the clay material could be repurposed. The estimated area of specialized excavation had a size of 17,000 m^2 (200 × 85 m) and a specified depth of several centimeters over the entire area. GPS-controlled excavators were proposed to excavate the contaminated top soil applying lean principles (reducing if possible any waste such as rework, too much, or too little excavation) and more accurate estimates. The general contractor asked the research team to conduct a performance analysis of the developed UAV system. As explained earlier, survey and documentation of results with a RTS-based surveying approach was compared to the automated UAV-direct geo-referenced mapping approach. Both results were referenced to a global coordinate system that was eventually used to control the excavating equipment. The following explains procedures and results.

(a) Field trial environment.
(b) Generating the point cloud from photos taken at waypoints.
(c) Detailed field-of-view: Terrain and pieces of equipment.
(d) Plan view of the generated orthophoto with the selected earth piles that were used for the comparative study.

The UAV survey was prepared as previously explained by (1) using indirect referencing by measuring and marking of eight ground control targets in the observation area using a GNSS receiver and SAPOS (German DGNSS Reference Station System) and (2) planning the flight trajectory with the developed flight planning tool and the following attributes: camera (Sony NEX5N with 16 mm fixed focal length), flying altitude of 70 m, longitudinal overlap 80%, and lateral overlap 60%.

Table 5
Survey results of RTS and UAV for three earth piles.

	Area	RTS		UAV		Error	
	[m^2]	[m^3]	Points	[m^3]	Points	[m^3]	[%]
Pile 1	443	730	29	789	3877	59	8%
Pile 2	440	997	40	1090	2617	93	9%
Pile 3	95	81	24	95	454	14	16%

A total of 64 images were recorded providing a ground resolution of 2 cm per pixel at an estimated mean error of 2 cm (horizontal) and 6 cm (vertical). A more detailed error analysis was performed in some of the selected excavation areas: these were a larger area (8300 m^2) and three smaller earth piles (see Fig. 7D). All were measured with a RTS and the UAV. The terrain did not change between both measurements. Potentially existing interferences from vegetation in both surveys were removed. Since the area was cleared already from trees and large bushes, this manual task took only a few minutes for both surveys. 3D surface models based on data from both survey methods were generated. The results were compared.

The points recorded and measured by the RTS and UAV were 202 and 122,275, respectively. The UAV data was used to first create an elevation map (in colors from blue (= lower) to red (= higher elevation)). The overlapping area between the RTS and UAV models was 7761 m^2. A triangulated surface mesh model was generated for each point cloud.

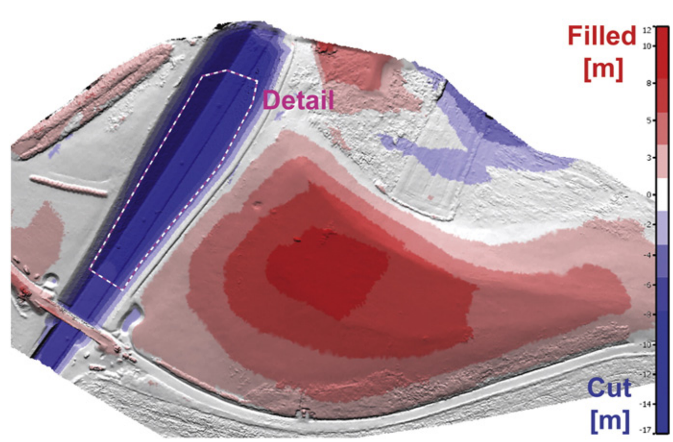

Fig. 9. Cut and fill documentation (location and heights) of already performed earthmoving operation for a high-speed rail project.

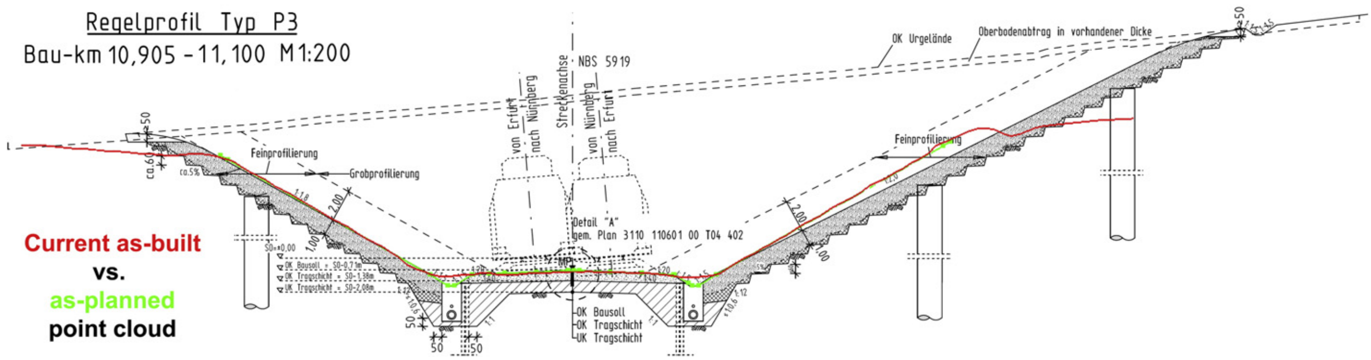

Fig. 10. Cross-sectional view in the area of interest showing current as-built project status vs. final as-planned project status.

Subtracting both models from each other resulted in a volume difference of 149 m^3 or an average height difference of 1.9 cm ($=149\ m^3/7761\ m^2$) and as an average value over the entire overlapping area.

Table 4 displays more results as they relate to the RTS and UAV comparison. It includes a comparison of how long each survey technique took. Since measurements using RTS and UAV were taken from 142 accessible locations on the project, the circles in Fig. 8 display at what locations (center of yellow circles) the error of the UAV system was high and small (large and small circles, respectively). The numbers in Fig. 8 indicate the differences in the elevation measurement. Negative and positive values indicate the UAV measured the point too low or too high, respectively. The average height error between the RTS and UAV measurements was 4.2 cm with a standard deviation of $\sigma = 5.9$ cm.

The UAV surface model was on average about 1.9 cm higher than the RTS surface model. Potential reasons for this observation are: (1) thickness of the ground control points (for example: reference targets had a height of 1 cm), (2) the general tendency of measuring too low with a RTS (for example: having the surveying pole/rod slightly penetrating the ground surface), (3) impact of vegetation and surface conditions (for example: areas with standing water that cannot or hardly be measured using a RTS), and (4) number of survey point (for example: a higher number of measured points eventually makes a UAV-based measurement technique more accurate since the measurement resolution is denser). The latter two reasons were specifically observed and noted in the field experiment.

For these reasons, three isolated earth piles (see Fig. 8) were measured in more detail. Results are shown in Table 5. The differences in the surveyed earth volumes for the three piles were between 8 and 16%. Since fewer points were taken with the RTS, it is assumed that the UAV measurement provides a more accurate earth volume estimate. However, to avoid over- and underestimating of the volumes a terrestrial dense point cloud laser scanning approach should have been utilized to compare the results more accurately. Although such alternative surveying methods need to be applied in future research, it may provide little practical value because earthwork estimating work which is conducted frequently through field inspection and personal site visits requires fast data collection and analysis. Most earth volume estimates today are measured with a RTS because it offers sufficiently accurate data for field practitioners. It is often preferred over laser scanning since it is less expensive, collects fewer points for data management, and is easier to setup and faster to perform.

8.3. Application in high-speed rail construction and spoil site projects

The UAV was also tested in two additional application areas: a high-speed rail construction project and a spoil site. Both assignments required the UAV to provide unique data that aids in construction engineering and management tasks.

The first assignment asked the survey team to use the UAV to provide survey data of an ongoing high-speed rail project in Germany (completion of the project numbered 8.1 as part of the German

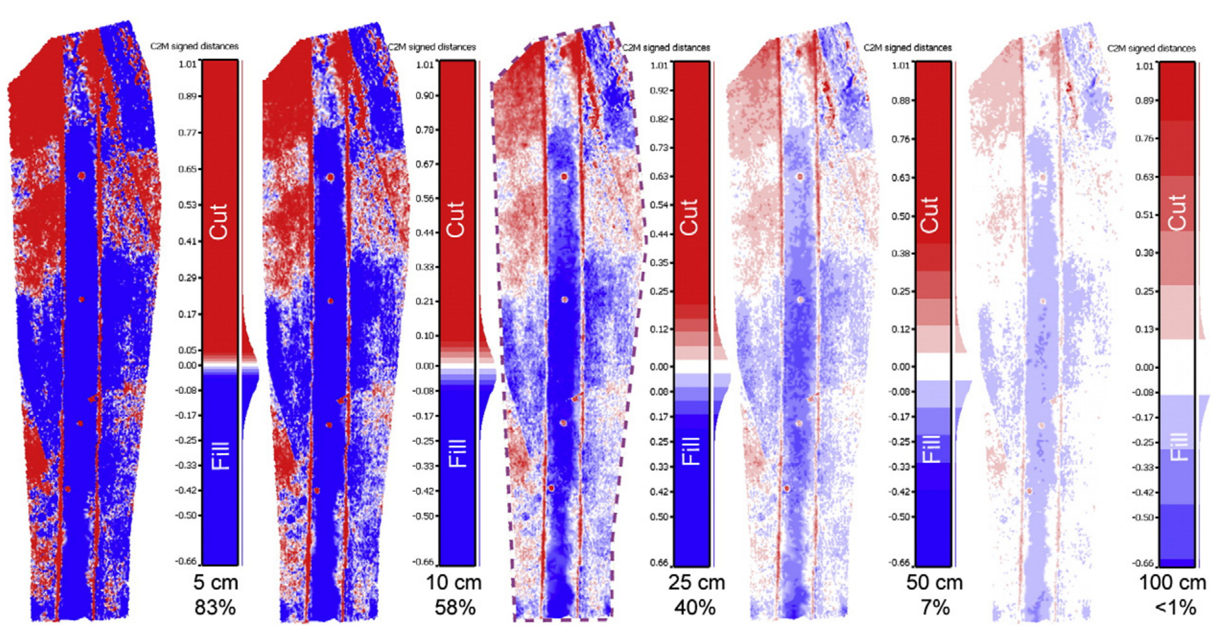

Fig. 11. Acceptable tolerances [in cm] for excavation area illustrate the locations and overall percentage of height change required.

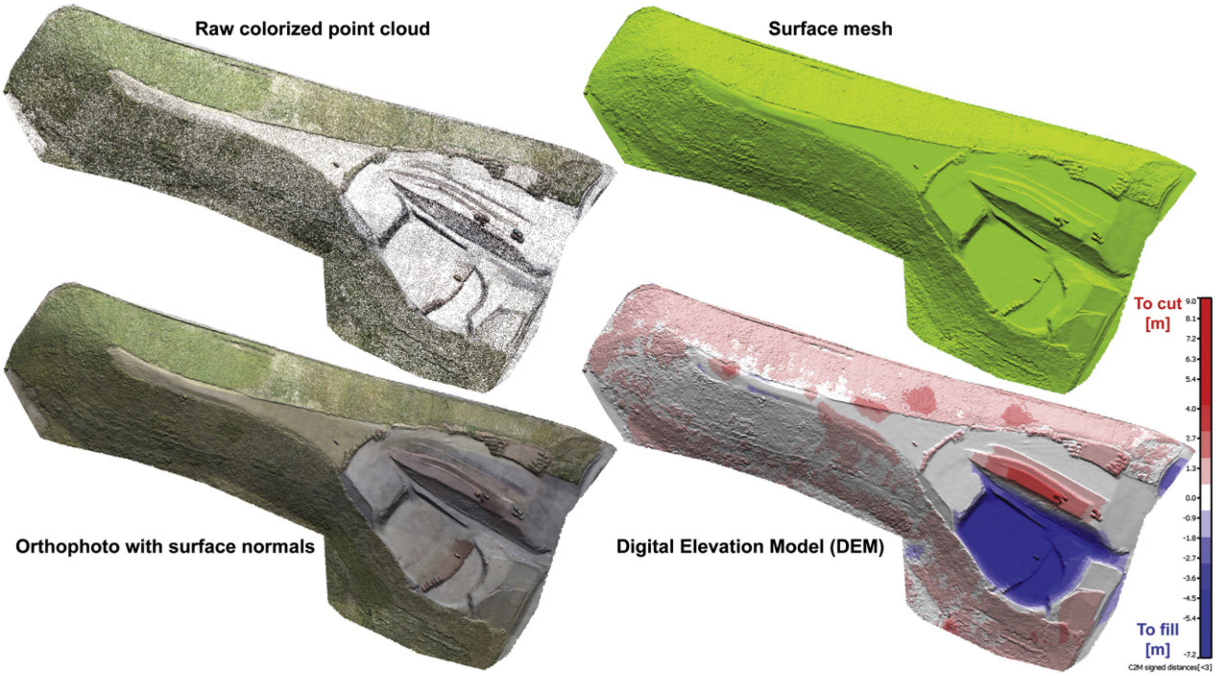

Fig. 12. Acceptable tolerances [in cm] for excavation area illustrate the locations and overall percentage of height change required.

reunification and rebuilding effort). A small segment of the track to be built from the cities Erfurt to Nuremberg was selected as it contained a cut and fill task. The length of the track section that was cut in open terrain was 330 m. The cut material (approximately 0.7 million m^3) was dumped next to the track to an acquired piece of land. Since the neighboring land was used for agricultural purposes, precise documentation of cut and fill locations and heights were mandated by the federal government. In addition, the owner and construction quality manager were in need of as-builts of ongoing earthwork and track building activities. They, in particular, were interested if milestones of building the track base were completed and at what locations and at what size deviations from as-planned models occurred.

The area of interest is shown in Fig. 9. Path of the track, spoil site, a bridge, and even some equipment was captured by the UAV data acquisition. The elevation view of the track is shown in Fig. 10. Two curves were plotted: one is the as-planned height of the final track base (before rail infrastructure was installed) and one is the as-built height. Please note, at the time of the UAV data acquisition the contractor was still performing height adjustments on site. This is why it was interesting for the construction manager to measure and see locations and heights of areas where the already performed earthmoving and compacting activities deviated from the plans. These deviations are illustrated in Fig. 11. Digital Elevation Models (DEM) allow to provide multiple views and generate reports that eventually are useful for practitioners. One example is shown in Fig. 11. Cut and fill areas become visible as they can be colored (here: red and blue, respectively). Even the drainage ditches on both sides of the railroad track (indicated in green in Fig. 10) and the manholes which still require excavation are visualized in Fig. 11 as vertical red lines and small red circles. Further analysis of the data set provides information that at least 83% of all work areas require work if the maximum acceptable height deviation shall be less or equal than 5 cm. Multiple of these percentages are provided as the heights are adjusted and although a high speed rail project may ultimately require millimeter accuracy, such visualized spatial information becomes useful in decision making in the field.

A spoil site is a location where earth material is temporarily stored for later use. Requirements to store the material are often similar to landfills, in particular for erosion and slope control. A spoil site for the high-speed rail project was selected. Its capacity was approximately 2 million m^3 at a length of 570 m, width of 170 m, and up to 25 m in height. As in the previous examples, the UAV collected the photos that generated the raw 3D point cloud. It was processed to a surface mesh and then to an orthophoto with surface normals. A Digital Elevation Model (DEM) was generated to illustrate the cut and fill status of the project. This was then compared to the as-planned model engineers built in advance of the project. Illustrated in Fig. 12 are all steps of the data acquisition and processing: raw colorized point cloud data, surface mesh, orthophoto with surface normals, and DEM. The DEM illustrates in colors the cut and fill areas and heights that are still to be performed. Highlighted in Fig. 13 are the DEM and the enlarged areas of interest.

The construction project manager's task was to determine at what time additional fill material was required to arrive at the spoil site. The following conditions existed at the time of decision making: The cut material which was still available had a surface area of 9136 m^2 and an in-situ volume of 5566 m^3. The fill area covered a surface area

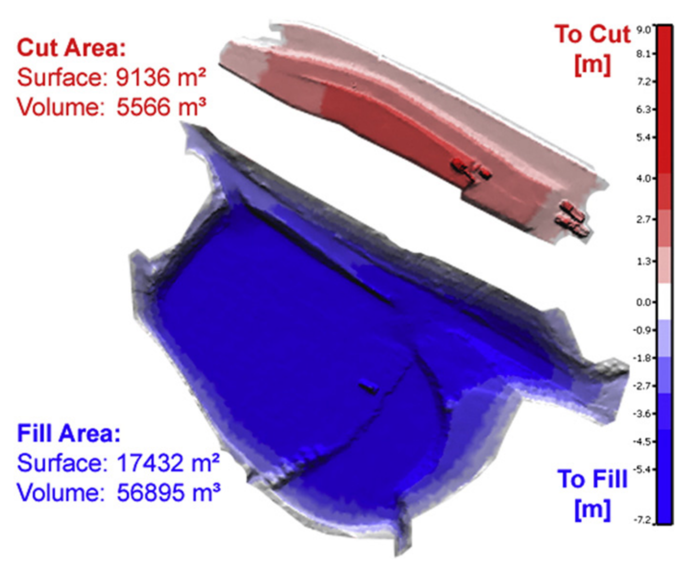

Fig. 13. Detail to cut and fill operation.

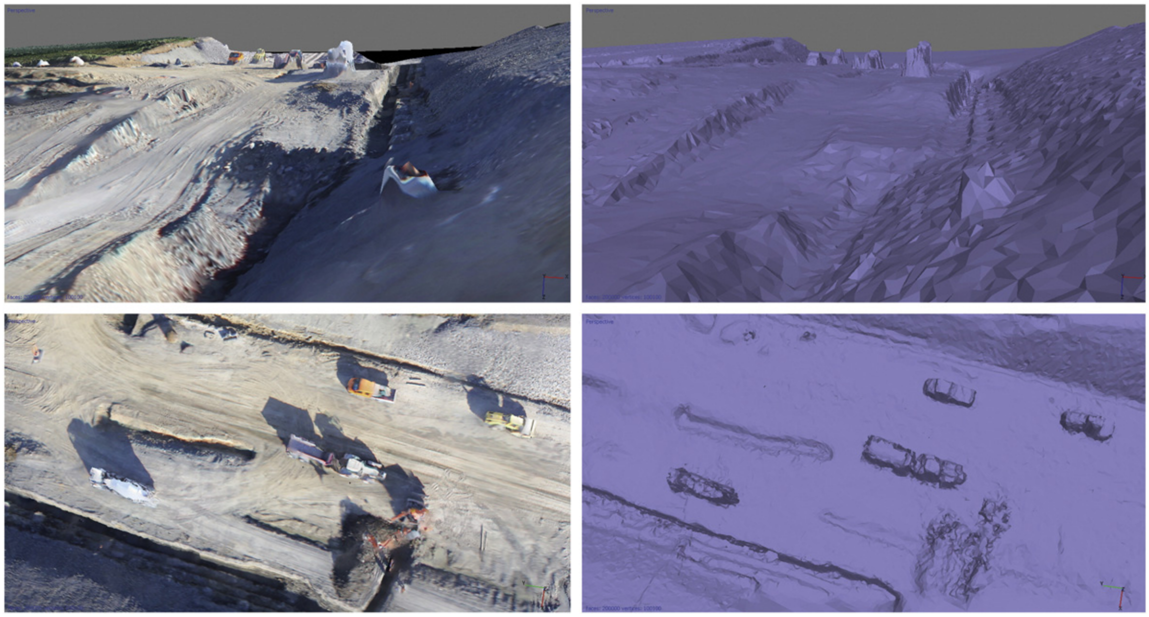

Fig. 14. Next steps in research: automated analysis of excavation parameters (slope and safety requirements) and construction equipment and earthwork progress tracking.

of 17,432 m^2 and required approximately 56,895 m^3 additional fill material to finish the project. All of these numbers were derived from the Digital Elevation Model (DEM) that originated from the UAV photo data. The cut material was sand and gravel (swell factor: approximately 1.15). The weather conditions were dry and the road conditions excellent. Enough capacity at the dump location was available to handle and compact the fill material. One excavator (1.5 m^3 bucket size; load time per truck: 5 min); and 7 dump trucks (maximum haul volume: 15 m^3) were available. The total travel time of each truck to the dump site and return to the load station was measured 13 min. The dump time calculated with 2 min. The effective work hours per truck driver and work day were 7 h (not including 1 hour total break time per day). During a work hour, each truck was able to complete 3 full trips (or 21 trips per each work day). The excavator would not idle should trucks not be available as it would prepare (loosen) the soil. On a few occasions the operator would take also the required break times. An estimated 701 truckloads were required, to cut, transport, and fill the available material. The calculated duration was 4.7 days, or practically 5 days or almost one full work week. Based on this simplified calculation and the data the UAV gathered, the project manager had enough information to accurately forecast that at the beginning of the next work week additional fill material would need to arrive to continue with the fill operation seamlessly. This information was helpful since otherwise the fill operation would have been interrupted, and potentially would have caused other delays for activities on the project's critical path.

Additional field applications of interest may result from fast UAV point cloud data acquisition (as shown in Fig. 14): automated planning of safety equipment necessary in embankment construction (trenches and slope classification) and automated construction equipment tracking, productivity or progress monitoring utilizing GPS and in addition spatial coordinates of work volumes accomplished per day [33,35,36].

Point cloud data acquisition through UAV may further yield a competitive data acquisition approach towards autonomous and automated point cloud to model conversion. Several recent and promising studies, including [37–41], show that 3D point clouds acquired by laser scanners, video or photo cameras positioned on the ground can be successfully converted to object models. Further research is necessary to fully automate the process for complex objects, and reduce error rates in point cloud to model conversion.

9. Conclusion

A novel approach was presented for evaluating the performance of a newly-designed and -built Unmanned Aerial Vehicle (UAV) system in test bed and field-realistic environments. The paper explained the hardware components as well as a novel flight path planning software tool that allows a pilot to launch the UAV for automated surveying tasks. The methodology on how photo images taken by a camera attached to the UAV were geo-referenced was explained. The UAV was evaluated in a test bed environment and its performance was assessed by comparing its results to other research publications. Furthermore, test trials in field-realistic environments were conducted to demonstrate the successful applicability of UAV and photogrammetric surveying for civil engineering applications. The evaluation focused in particular on the magnitude of the errors of a UAV-based photogrammetric approach as it compares to conventional surveying techniques that were used for ground truth measurements. Factors and errors influencing UAV-based photogrammetric measurements were defined and discussed. Results of these tests demonstrate improvements compared to previous research. However, some technical limitations of current UAV systems may need resolution, such as the battery life limiting its flight duration. Future work may also address more case studies when using UAV or alike UAS or RPV systems in the harshest possible work environments and carrying varies types of additional sensors, for example, range or infrared.

References

[1] GPS, Data From the First Week Without Selective Availability, http://www.gps.gov/systems/gps/modernization/sa/data/2000 (Accessed January 15, 2013).

[2] H. Eisenbeiß, UAV Photogrammetry, Dissertation Institute of Geodesy and Photogrammetry, ETH Zurich, Switzerland, 2009.

[3] H. Saari, T. Antila, C. Holmlund, J. Mäkynen, K. Ojala, H. Toivanen, I. Pellikka, S. Tuominen, L. Pesonen, J. Heikkilä, Unmanned Aerial Vehicle (UAV) operated spectral camera system for forest and agriculture applications, Proc. SPIE 8174 (2011).

[4] A. Rango, A. Laliberte, C. Steele, J.E. Herrick, B. Bestelmeyer, T. Schmugge, A. Roanhorse, V. Jenkins, Using unmanned aerial vehicles for rangelands: current applications and future potentials, Environ. Pract. 8 (3) (2006) 159–168.

[5] E. Semsch, M. Jakob, D. Pavlicek, M. Pechoucek, Autonomous UAV surveillance in complex urban environments, IEEE/WIC/ACM International Joint Conferences on Web Intelligence and Intelligent Agent Technologies, 2, WI-IAT, 2009, pp. 82–85.

[6] M. Kontitsis, N. Tsourveloudis, K.P. Valavanis, A UAV vision system for airborne surveillance, Proceedings IEEE International Conference on Robotics and Automation, New Orleans, LA, 1, 2004, pp. 77–83.

[7] B. Ameri, D. Meger, K. Power, Y. Gao, UAS applications: disaster and emergency management, Proceedings of America Society of Photogrammetry and Remote Sensing Annual Conference, Baltimore, MD, CD ROM, 2008.
[8] F. Heintz, P. Rudol, P. Doherty, From images to traffic behavior—a UAV tracking and monitoring application, 10th International Conference on Information Fusion, IEEE, 2007.
[9] S. Srinivasan, H. Latchman, J. Shea, T. Wong, J. McNair, Airborne traffic surveillance systems: video surveillance of highway traffic, Proceedings of the ACM 2nd international workshop on Video surveillance & sensor networks, 2004.
[10] A. Puri, A Survey of Unmanned Aerial Vehicles (UAV) for Traffic Surveillance, Department of Computer Science and Engineering, University of South Florida, 2005.
[11] F. Remondino, L. Barazzetti, F. Nex, M. Scaioni, D. Sarazzi, UAV photogrammetry for mapping and 3D modeling–current status and future perspectives, in: H. Eisenbeiss, M. Kunz, H. Ingensand (Eds.), Proceedings of the International Conference on Unmanned Aerial Vehicle in Geomatics (UAV-g) 2011, Zurich, Switzerland, September 2011.
[12] L.I.N. Zongjian, UAV for mapping—low altitude photogrammetric survey, International Archives of Photogrammetry and Remote Sensing, Beijing, China, 2008.
[13] D. Hausamann, W. Zirnig, G. Schreier, P. Strobl, Monitoring of gas pipelines—a civil UAV application, Aircr. Eng. Aerosp. Technol. 77 (5) (2005) 352–360.
[14] B.P. Hudzietz, S. Saripalli, An experimental evaluation of 3d terrain mapping with an autonomous helicopter, in: H. Eisenbeiss, M. Kunz, H. Ingensand (Eds.), Proceedings of the International Conference on Unmanned Aerial Vehicle in Geomatics (UAV-g) 2011, Zurich, Switzerland, September 2011.
[15] D. Bulatov, P. Solbrig, H. Gross, P. Wernerus, E. Repasi, C. Heipke, Context-based urban terrain reconstruction from UAV-videos for geoinformation applications, in: H. Eisenbeiss, M. Kunz, H. Ingensand (Eds.), Proceedings of the International Conference on Unmanned Aerial Vehicle in Geomatics (UAV-g) 2011, Zurich, Switzerland, September 2011.
[16] F. Neitzel, J. Klonowski, Mobile 3D mapping with a low-cost UAV system, Int. Arch. Photogramm. Remote. Sens. Spat. Inf. Sci. 38 (2011) 1–6.
[17] W. Jizhou, L. Zongjian, L. Chengming, Reconstruction of buildings from a single UAV image, Proc. International Society for Photogrammetry and Remote Sensing Congress, 2004, pp. 100–103.
[18] C. Wefelscheid, R. Hansch, O. Hellwich, Three-dimensional building reconstruction using images obtained by unmanned aerial vehicles, in: H. Eisenbeiss, M. Kunz, H. Ingensand (Eds.), Proceedings of the International Conference on Unmanned Aerial Vehicle in Geomatics (UAV-g) 2011, Zurich, Switzerland, September 2011.
[19] N. Metni, T. Hamel, A UAV for bridge inspection: visual servoing control law with orientation limits, Automation in Construction, 17 (1), Elsevier, 2007. 3–10.
[20] S. Rathinam, Z.W. Kim, R. Sengupta, Vision-based monitoring of locally linear structures using an unmanned aerial vehicle, First J. Infrastruct. Syst. 14 (1) (2008) 52–63.
[21] J. Gao, Y. Yan, C. Wang, Research on the application of UAV remote sensing in geologic hazards investigation for oil and gas pipelines, ASCE ICPTT 2011@ Sustainable Solutions For Water, Sewer, Gas, And Oil Pipelines, 2011, pp. 381–390.
[22] C. Zhang, A. Elaksher, An unmanned aerial vehicle based imaging system for 3D measurement of unpaved road surface distresses, J. Comput. Aided Civ. Infrastruct. Eng. 27 (2) (2011) 118–129.
[23] J. Irizarry, M. Gheisari, B.N. Walker, Usability assessment of drone technology as safety inspection tools, ITcon 17 (2012) 194–212.
[24] Mikrokopter, Website http://www.mikrokopter.de2012 (Accessed, June 15, 2012).
[25] D. Lowe, Distinctive image features from scale-invariant keypoints, Int. J. Comput. Vis. 60 (2) (2004) 91–110.
[26] N. Snavely, S.M. Seitz, R. Szeliski, Modeling the world from internet photo collections, Int. J. Comput. Vis. 80 (2) (2007) 189–210.
[27] Y. Furukawa, B. Curless, S.M. Seitz, R. Szeliski, Towards Internet-scale multi-view stereo, IEEE Conference on Computer Vision and Pattern Recognition (CVPR), 2010, pp. 1434–1441.
[28] Y. Furukawa, J. Ponce, Accurate, dense, and robust multiview stereopsis, IEEE Trans. Pattern Anal. Mach. Intell. 32 (8) (2010) 1362–1376.
[29] AgiSoft PhotoScan, Website http://www.agisoft.ru2012 (Accessed June 25, 2012).
[30] F. Neitzel, J. Klonowski, S. Siebert, J. Dasbach, Mobile 3D Mapping mit einem low-cost UAV-System am Beispiel der Deponievermessung, Proceedings of Oldenburger 3D Tage (Photogrammetrie Laserscanning Optische 3D-Messtechnik), Wichmann Herbert, 2011, pp. 300–311.
[31] J. Teizer, B.S. Allread, C.E. Fullerton, J. Hinze, Autonomous pro-active real-time construction worker and equipment operator proximity safety alert system, Automation in Construction, 19 (5), Elsevier, 2010. 630–640.
[32] J.W. Hinze, J. Teizer, Visibility-related fatalities related to construction equipment, Journal of Safety Science, 49 (5), Elsevier, 2011. 709–718.
[33] S. Zhang, J. Teizer, J.K. Lee, C. Eastman, M. Venugopal, Building Information Modeling (BIM) and safety: automatic safety checking of construction models and schedules, Automation in Construction, 29, Elsevier, 2013. 183–195.
[34] E. Marks, J. Teizer, Method for testing proximity detection and alert technology for safe construction equipment operation, Construction Management and Economics, Special Issue on Occupational Health and Safety in the Construction Industry, 31(6), Taylor & Francis, 2013. 636–646.
[35] N. Pradhananga, J. Teizer, Automatic spatio-temporal analysis of construction equipment operations using GPS data, Automation in Construction, 29, Elsevier, 2013. 107–122.
[36] J. Melzner, S. Zhang, J. Teizer, H.-J. Bargstädt, Quantification and visualization of U.S. and German fall protection standards using automated safety-rule checking in Building Information Models (BIM), Construction Management and Economics, Special Issue on Occupational Health and Safety in the Construction Industry, 31(6), Taylor & Francis, 2013. 661–674.
[37] F. Bosché, C.T. Haas, Automated retrieval of 3D CAD model objects in construction range images, Autom. Constr. 17 (4) (2008) 499–512.
[38] F. Bosché, Automated recognition of 3D CAD model objects in laser scans and calculation of as-built dimensions for dimensional compliance control in construction, Advanced Engineering Informatics, 24(1), Elsevier, 2010. 107–118.
[39] P. Tang, D. Huber, B. Akinci, R. Lipman, A. Lytle, Automatic reconstruction of as-built building information models from laser-scanned point clouds: a review of related techniques, Automation in Construction, 19, Elsevier, 2011. 829–843.
[40] M. Golparvar-Fard, J. Bohn, J. Teizer, S. Savarese, F. Peña-Mora, Evaluation of image-based modeling and laser scanning accuracy for emerging automated performance monitoring techniques, Automation in Construction, 20(8), Elsevier, 2011. 1143–1155.
[41] G. Zhang, P.A. Vela, I. Brilakis, P. Karasev, A sparsity-inducing optimization based algorithm for planar patches extraction from noisy point-cloud data, Computer-Aided Civil and Infrastructure Engineering, Wiley, 2014. (in print).